

# Some Design Considerations for Embankments on Rate Sensitive Soils

Allen Lunzhu Li<sup>1</sup> and R. Kerry Rowe, F.ASCE<sup>2</sup>

**Abstract:** Both the short-term and long-term behavior of reinforced embankments constructed on rate sensitive foundation soils is investigated. Factors such as the rate sensitive properties of the foundation soil, reinforcement stiffness, construction rates, and different foundation soil profiles are considered. The strain rate at which the foundation soils deform during and after embankment construction is examined. For embankments on these soils the analysis indicates that the critical stage with respect to stability occurs during a period of creep and stress relaxation in the foundation soils after construction. The strain rate corresponding to this critical stage controls the operational shear strength of rate sensitive foundation soils and this strain rate falls into a relatively small range of values for the wide range of conditions examined. A technique that allows a conventional undrained limit equilibrium analysis to be modified to allow the design of reinforced embankments over rate sensitive foundation soils is proposed based on the critical stage concept.

**DOI:** 10.1061/(ASCE)1090-0241(2002)128:11(885)

**CE Database keywords:** Soft soils; Reinforcement; Embankments; Creep; Design; Stress relaxation.

## Introduction

The effect of time (strain rate) on the strength of soft cohesive soils has been extensively investigated since the early work of Terzaghi (1931) and Casagrande and Wilson (1951). Terzaghi (1931) stressed the importance of the consideration of the rate effects on the shear strength of clays in the design of foundations. Experimental results have consistently shown that the loading rate has an effect on the undrained shear strength and that stress-strain relations of natural soft clays are strain rate dependent (Perloff and Osterberg 1963; Bjerrum 1972; Lo and Morin 1972; Graham et al. 1983; Kulhawy and Mayne 1990; Leroueil and Marques 1996). Bjerrum (1973) attributed the time effect to the “interparticle creep” along the direction of shear due to the presence of the viscous adsorbed water between clay particles. The undrained creep during shear in the soil gives rise to increased pore pressures, decreased effective stresses, and decreased strengths; consequently, the undrained shear strength is rate dependent (Ladd and Foott 1974).

Due to the viscous nature of some soft clayey foundations, embankments on these soils may experience significant post construction creep deformations or even failure when excess pore pressures increase or remain at a nearly constant level following

the completion of construction (Lo et al. 1976; Fisher et al. 1982; Crooks et al. 1984; Kabbaj et al. 1988; Rowe et al. 1996). Kabbaj et al. (1988) reported (Fig. 1) that the observed excess pore pressure at location G3 at the Berthierville test site increased by 14 kPa during the first 39 days after the end of construction of a 2.4-m-high circular test embankment and the excess pore pressure at location G1 continued to increase until 140 days after the end of construction. At another test embankment site (Moncton, New Brunswick, Canada), unusually high-excess pore pressures were reported even three years after the end of construction of a 4.4-m-high embankment on an organic silty clay deposit (Keenan et al. 1986). It is worth noting that while the excess pore pressure may increase slightly due to the Mandel-Cryer effect over relatively short periods immediately after the end of embankment construction (Schiffman et al. 1969), the response observed in this case (Fig. 1) does not appear consistent with this being the sole explanation for the observed buildup in pore pressure.

The construction of reinforced embankments needs special consideration when the foundation soil exhibits an increase in undrained shear strength of 10% or greater for one order of magnitude increase in strain rate (Li 2000). Under these circumstances, the strain in the reinforcement at a constant fill thickness can significantly increase due to the creep of the rate sensitive foundation soil. For example, in the Sackville reinforced embankment case, the strain gauges attached to the geotextile reinforcement recorded an increase of reinforcement strain from 2.5 to 5.0% during a 15-h period at a constant fill thickness of 5.7 m (Gnanendran 1993). The rate sensitive characteristics of soft foundation soils can have significant influence on the behavior of reinforced embankments (Rowe and Hinchberger 1998; Li 2000; Rowe and Li 2000). Due to the paucity of studies into the effect of the viscous behavior of rate sensitive cohesive soils on the performance of reinforced embankments, current design methods (Jewell 1982; Leshchinsky 1987; Holtz et al. 1997; Koerner 1997; and others) do not allow for this effect.

Undrained stability analyses have been extensively developed and widely used in design (Bjerrum 1972; Ladd and Foott 1974; Trak et al. 1980; Ladd 1991). Direct (uncorrected) use of the

<sup>1</sup>Postdoctoral Fellow, GeoEngineering Centre at Queen's-RMC, Dept. of Civil Engineering, Queen's Univ., Kingston ON, Canada K7L 3N6.

<sup>2</sup>Professor and Vice-Principal (Research), Queen's Univ., Kingston ON, Canada K7L 3N6 (corresponding author). E-mail: kerry@civil.queensu.ca

Note. Discussion open until April 1, 2003. Separate discussions must be submitted for individual papers. To extend the closing date by one month, a written request must be filed with the ASCE Managing Editor. The manuscript for this paper was submitted for review and possible publication on February 13, 2001; approved on March 22, 2002. This paper is part of the *Journal of Geotechnical and Geoenvironmental Engineering*, Vol. 128, No. 11, November 1, 2002. ©ASCE, ISSN 1090-0241/2002/11-885-897/\$8.00+\$0.50 per page.

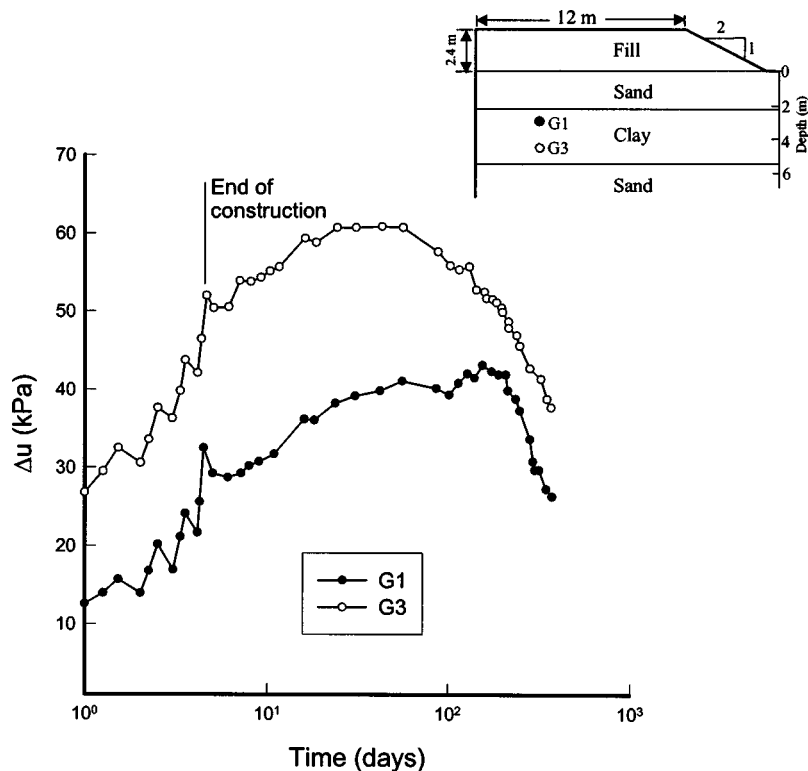


Fig. 1. Variation in excess pore pressure with time at Berthierville test site (modified from Kabbaj et al. 1988)

undrained shear strength of soil measured in the laboratory or in situ at currently recommended strain rates may lead to potential postconstruction failure (Rowe and Li 2000). Correlations of strain rate and undrained shear strength have been proposed (Kulhawy and Mayne 1990; Soga and Mitchell 1996). However, the in situ strain rate has not been well defined and hence difficult to account for in design. An empirical correction factor has been proposed to consider rate effects (Bjerrum 1973; Dascal and Tournier 1975) on the undrained shear strength measured using a field vane test although this approach has been controversial (Schmertmann 1975; Larsson 1980; Graham et al. 1983).

The objective of this paper is to provide insight regarding the behavior of reinforced embankments constructed over rate sensitive soils by using the results of finite-element (FE) analyses to gain insight regarding the in situ strain rate beneath a reinforced embankment. The factors considered include the viscoplastic properties of the foundation soil, reinforcement stiffness, construction rates, and different foundation soil profiles. Particular attention is given to identifying: (1) the point (called the critical stage) at which instability is most likely; (2) the strain rates at which the foundation deforms; and (3) the operational shear strength of foundation soils under embankment loading. This information will then be used to provide a means of estimating the shear strength that can be used in the design of a reinforced embankment on these soils.

### Behavior of Rate Sensitive Cohesive Soils and Constitutive Model

In laboratory undrained compression and consolidation tests, the rate sensitive behavior of soft cohesive soils can be manifest in terms of the effect of the rate of loading on the measured undrained shear strength, the preconsolidation pressure, and the

stress-strain curve of the soil (Leroueil 1985; Soga and Mitchell 1996). Graham et al. (1983) observed that the increase in undrained shear strength was between 10 and 20% per logarithmic cycle of strain rate for a number of soft clays. Kulhawy and Mayne (1990) reported an average gradient of 10% per log cycle of strain rate based on data for 26 clays from different regions. Fig. 2(a) shows the effect of strain rate on the undrained stress paths during anisotropically consolidated undrained compression tests on the clayey silt from the Sackville test site in Canada (Hinchberger 1996). It shows that the increase of strain rate from 0.1 to 1.14%/min resulted in an increase in undrained shear strength by 14%. As another example, Sheahan et al. (1996) showed significant rate dependence of the undrained shear strength of resedimented Boston Blue clay [Fig. 2(b)]. Soga and Mitchell (1996) conducted undrained triaxial compression tests on the structured Pancone clay from Pisa, Italy and the stress strain curves at constant strain rates of 0.05 and 0.005 %/min were significantly different. However, Berre and Bjerrum (1973) have also suggested that there is a threshold strain rate below which the shear strength dependence on strain rate can decrease significantly.

The constitutive model of the foundation soil used in numerical analyses should have the capability to capture the main characteristics of rate sensitive soils noted above, including rate dependence of undrained shear strength and creep-induced excess pore pressures. In this study, an elastoviscoplastic soil model with these capabilities (Rowe and Hinchberger 1998) is used to describe the time-dependent behavior of the soft foundation soils. This soil model is based on Perzyna's theory of overstress viscoplasticity (Perzyna 1963) and an elliptical yield cap model proposed by Chen and Mizuno (1990). Perzyna's viscoplastic theory is well established and can describe much of the rate sensitive behavior of soils and rocks (Adachi and Oka 1982; Katona and

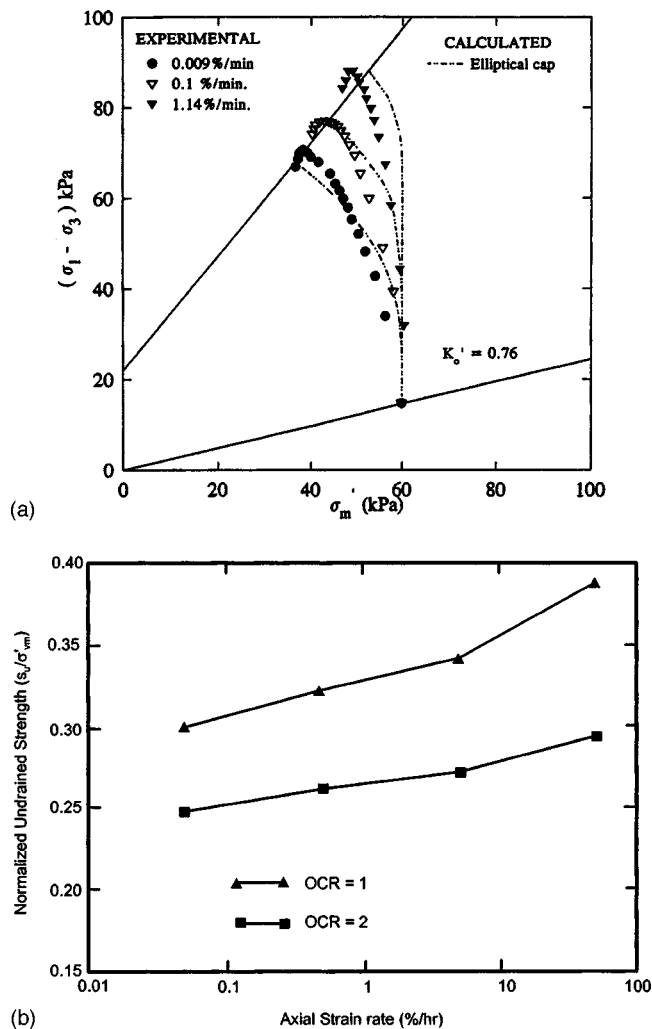


Fig. 2. Behavior of soft rate sensitive soils

Mulert 1984; Desai and Zhang 1987). The elliptical cap model which allows consideration of the variation of yield surface between different soils, has been widely used to describe the yield behavior of soils (Katona and Mulert 1984; McCarron and Chen 1987; Humphrey and Holtz 1988; Chen and Mizuno 1990; Huang and Chen 1990). For example, Fig. 2(a) shows good agreement between measured and calculated stress paths at different strain rates obtained using the proposed model for the Sackville soil.

Using this viscoplastic cap model, Rowe and Hinchberger successfully described the short-term behavior of a reinforced embankment constructed over Sackville foundation soil (Rowe and Hinchberger 1998) and long-term behavior of an unreinforced embankment constructed over Gloucester foundation soil (Hinchberger and Rowe 1998). Briefly, the elliptical cap yield envelope is defined in terms of an aspect ratio  $R$  and the failure is governed by the Drucker-Prager failure envelope having a slope  $M_{N/C}$  and  $M_{O/C}$  for the normally and overconsolidated failure, respectively. Other key parameters include the compression index ( $\lambda$ ) and recompression index ( $\kappa$ ), the initial void ratio ( $e_0$ ), the preconsolidation pressure ( $\sigma'_p$ ), the coefficient of earth pressure at rest ( $K_o$ ), Poisson's ratio ( $\nu'$ ), the unit weight of the soil ( $\gamma$ ), and the hydraulic conductivity of the soil ( $k$ ). The viscoplastic nature of the soil is defined in terms of a viscoplastic fluidity parameter  $\gamma^{VP}$  and a strain rate exponent,  $n$ , as described by Rowe and Hinchberger (1998). The plastic strain follows an associated flow rule

which allows the modeling of positive volumetric plastic strain (compression) for soil yielding in a normally consolidated stress range, and negative volumetric plastic strain (dilation) for soil yielding in an overconsolidated stress range, and deformations at a constant volume at the critical state. It is noted that for the viscoplastic elliptical cap model, the parameter  $\gamma^{VP}$  corresponds to the strain rate below which soil is no longer rate sensitive (Katona and Mulert 1984). At the limit where  $\gamma^{VP} = \infty$ , the elastoviscoplastic model reduces to the elastoplastic model (Perzyna 1963). The lower the parameter  $n$ , the more rate sensitive the soil. For example, if two soils with the same elliptical cap soil properties (including the static preconsolidation pressures) are under undrained compression at a same strain rate, the soil with lower  $\gamma^{VP}$  and lower  $n$  will have higher-dynamic undrained shear strength.

## Finite-Element Modeling and Model Parameters

A version of the finite-element program *AFENA* (Carter and Baalam 1990) modified to incorporate an elastoviscoplastic elliptical cap soil model fully coupled with Biot consolidation theory (Biot 1941) was adopted in the analyses. An elastoplastic model with Mohr-Coulomb failure surface and a nonassociated flow rule proposed by Davis (1968) was adopted for the granular embankment fill. The nonlinear variation of granular soil stiffness with increasing stress level during construction was based on Janbu's equation (Janbu 1963). The geosynthetic reinforcement was considered using elastic one-dimensional bar elements. The interaction between the soil mass and the reinforcement was modeled by introducing soil-reinforcement interface elements with strength governed by Mohr-Coulomb failure criterion (Rowe and Soderman 1987). This finite-element program has been validated against a number of field embankments including the Almere reinforced embankment (Rowe and Soderman 1984), the Hubrey Road reinforced embankment (Rowe and Mylleville 1996), the Sackville reinforced embankment (Rowe and Hinchberger 1998), and the Gloucester embankment (Hinchberger and Rowe 1998).

The embankments examined in this paper have  $2h:1v$  side slopes and overlie a 15-m-soft cohesive deposit underlain by a relatively permeable and rigid layer. A total of 1,594 linear strain triangular elements (3,516 nodes) were used to discretize the embankment and foundation soils in a finite-element mesh that examined half of the geometry by taking account of symmetry. The centerline of the embankment and the far field lateral boundary were taken to be smooth and rigid and the lateral boundary was located 100 m from the centerline. The zero displacement and excess pore pressures were assigned to the nodes along the bottom boundary. Embankment construction was simulated by turning on the gravity of the embankment in 0.75-m-thick lifts at a rate corresponding to the embankment construction rate.

Three soft foundation soil profiles, denoted as Soils A, B, and C with three sets of viscoplastic properties, denoted as R1, R2, and R3, are examined in this paper. For example, the designation "Soil C-R1" means this foundation soil has elastoplastic properties of Soil C and viscoplastic properties of R1. The majority of the results presented here are based on Soil C having viscoplastic properties R1 ( $n=20$  and  $\gamma^{VP}=2 \times 10^{-5}/h$ ) or R2 ( $n=30$  and  $\gamma^{VP}=1 \times 10^{-7}/h$ ). The parameters for Soils A, B, and C are summarized in Table 1 and the preconsolidation pressure and initial vertical stress profiles are shown in Fig. 3. Both Soils A ( $W_L=76\%$ ,  $I_p=40\%$ ) and B ( $W_L=48\%$ ,  $I_p=30\%$ ) were slightly overconsolidated with an overconsolidation ratio (OCR) of 1.1 to

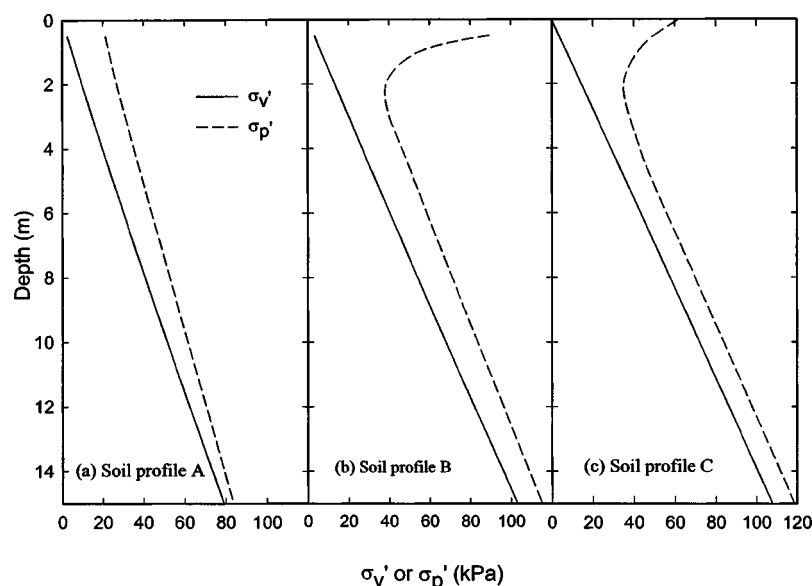
**Table 1.** Soil Model Parameters

	Soil A	Soil B	Soil C
Failure envelope $M_{N/C}$ ( $\phi'$ )	0.874(27°)	0.91(28°)	0.96(29°)
Failure envelope $M_{O/C}$	0.63	0.75	0.75
Aspect ratio $R$	0.7	1.25	1.25
Compression index $\lambda$	0.3	0.15	0.16
Recompression index $\kappa$	0.03	0.025	0.034
Coefficient of earth pressure at rest $K'_0$	0.6	0.6	0.75
Poisson's ratio $\nu'$	0.35	0.35	0.3
Unit weight $\gamma$ (kN/m <sup>3</sup> )	15.2	16.7	17
Initial void ratio $e_o$	2.03-2.5	1.31-1.5	1.38-1.5
Reference hydraulic conductivity $k_{vo}$ (m/s)	$1 \times 10^{-9}$	$1 \times 10^{-9}$	$2 \times 10^{-9}/4 \times 10^{-10}$
Change index $C_k$	1.25	1.25	0.2
Ratio $k_h/k_v$	3	3	4
Liquid limit $w_L$ (%)	76	48	50
Plasticity index $I_p$ (%)	40	30	18

2.6 and 1.1 to 2.9, respectively, below the first two meters. Soil B with a 2-m crust has a higher-preconsolidation pressure than Soil A. Soil C-R1 had properties similar to Sackville soil described by Rowe and Hinchberger (1998) with a liquid limit  $W_L$ , of 50%, plasticity index  $I_p$  of 18%, and natural water content of 53%, and an OCR of 2.4 to 1.1 below the first two meters. The increase in undrained shear strength of Soil C-R1 was about 16% per logarithm cycle of strain rate for strain rates between 0.005%/h and 100%/h, as shown in Fig. 4. This rate sensitivity fell into the range observed by Graham et al. (1983) for a number of cohesive soils (10–20% increase of strength per log cycle of strain rate). The shear strength was insensitive to strain rate for strain rates less than 0.002%/h (which was equal to the viscoplastic fluidity parameter,  $\gamma^{vp}$ ). Soil C-R2 had the same properties as Soil C-R1 except for the viscoplastic parameters. The increase in undrained shear strength of Soil C-R2 with strain rate had a similar magnitude to the average rate reported by Kulhawy and Mayne (1990) from 26 different clays (10% per logarithm cycle of strain rate) as shown in Fig. 4. The hydraulic conductivity of soft clays was taken to be a function of void ratio as proposed by Taylor (1948)

(i.e., a linear relationship between the logarithm of  $k$  and void ratio). The values for the reference hydraulic conductivity  $k_{vo}$ , and the change index  $C_k$  are shown in Table 1. The anisotropy of the hydraulic conductivity is considered by using the ratio of horizontal to vertical hydraulic conductivity,  $k_h/k_v$  (Table 1).

The embankment fill was assumed to be a purely frictional granular soil with a friction angle  $\phi' = 37^\circ$ , dilatancy angle  $\psi = 6^\circ$ , and a unit weight  $\gamma = 20$  kN/m<sup>3</sup>. The nonlinear elastic behavior of the fill was modeled using Janbu's (1963) equation with material constants  $K$  and  $m$  of 300 and 0.5, respectively. Rigid-plastic joint elements (Rowe and Soderman 1987) used for the fill/reinforcement interface were assumed to be frictional with  $\phi' = 37^\circ$ . An interface friction angle between fill and reinforcement of  $32^\circ$  was also examined and no slippage between the soil and reinforcement was observed. The elastic deformations of the joint elements were negligible. The fill/foundation interface had the same shear strength as that of the foundation soil at the ground surface. Reinforcement with tensile stiffness  $J$ , varying from 0 (no reinforcement) to 4,000 kN/m was examined. The focus of the present study is on reinforcement that is not particu-

**Fig. 3.** Preconsolidation pressure and initial vertical effective stress profiles of soil profiles A, B, and C

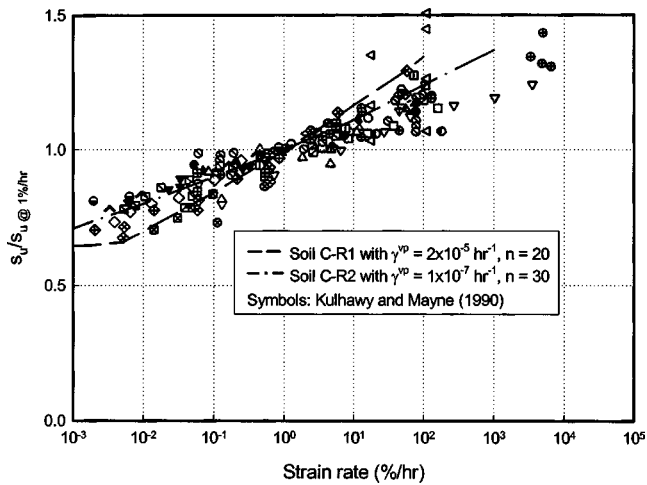


**Fig. 4.** Effect of strain rate on undrained shear strength  $s_u$  of Soils C-R1 and C-R2

larly rate sensitive at working stress levels, (e.g., polyester), and does not consider the effect of the time-dependent behavior of viscoelastic geosynthetic reinforcement, such as high-density polyethylene geogrids.

## Results and Discussion

### Strain Rate and Shear Strength Mobilized during Embankment Construction

In order to account for the strain rate effect on the behavior of reinforced embankments in the design, it is necessary to have some insight regarding the strain rates mobilized in the foundation soil during and following construction. To address this issue, the strain rate of the rate sensitive foundation soils below embankments is calculated numerically in this paper with a focus on the failure zone. Fig. 5 shows the calculated strain rate contours for the major principal strain at the onset of failure for an unreinforced embankment constructed at a rate of 10 m/month on Soil C-R1. The strain rate contours can be associated with a circular-

like failure surface. At failure, the soil along the failure surface deforms at a different, higher rate than the adjacent soil. The strain rate of Point A at the midpoint along the failure surface approximately represents the average velocity at which the foundation deforms at failure. Therefore, Point A can be considered as the representative point on a potential failure surface.

Fig. 6 shows how the strain rate at the representative Point A varies during embankment construction at a constant rate CR of 10 m/month. In the case of an embankment over Soil C-R1, the strain rate initially increased slowly up to a fill thickness of 2.3 m and then increased significantly with the fill thickness when the foundation soil behaved viscoplastically for a fill thickness greater than 2.3 m. The strain rate at embankment failure ( $H_f=6.15$  m) was  $5.7 \times 10^{-3}/h$ . For the case of an embankment over Soil C-R2, the strain rate increased significantly after 4 m of fill had been placed and the strain rate at embankment failure ( $H_f=7.43$  m) was  $5.9 \times 10^{-3}/h$ .

To evaluate the mobilized undrained shear strength during construction, a limit-equilibrium (LE) analysis was conducted using the calculated undrained shear strength profile of the foundation soil developed at a strain rate of  $5.7 \times 10^{-3}/h$  and  $5.9 \times 10^{-3}/h$  for Soils C-R1 and C-R2, respectively. The calculated equilibrium ratio ERAT (defined as the resisting moment divided by the disturbing moment) was 0.96 and 0.91 for the failure height of 6.15 m over Soil C-R1 and 7.43 m over Soil C-R2, respectively. This indicates that the undrained shear strength, calculated using the strain rate at Point A at failure, have reasonably represented the mobilized shear strength at embankment failure. Fig. 6 also shows the average vertical strain rate (the settlement with respect to time divided by the thickness of the foundation) at failure was about 6.5 times lower than the major principal strain rate at Point A for both cases. This indicates that the strain calculated in terms of settlement divided by foundation thickness only represents an average vertical strain rate throughout the deposit and does not represent the effect of shearing intensity and direction along the failure surface.

For the final embankment thickness as examined here (6.15 m over Soil C-R1 and 7.43 over Soil C-R2), the embankments were just stable at the end of construction, however, progressive failure occurred following the completion of construction due to creep and stress relaxation of foundation soil as shown by Li (2000).

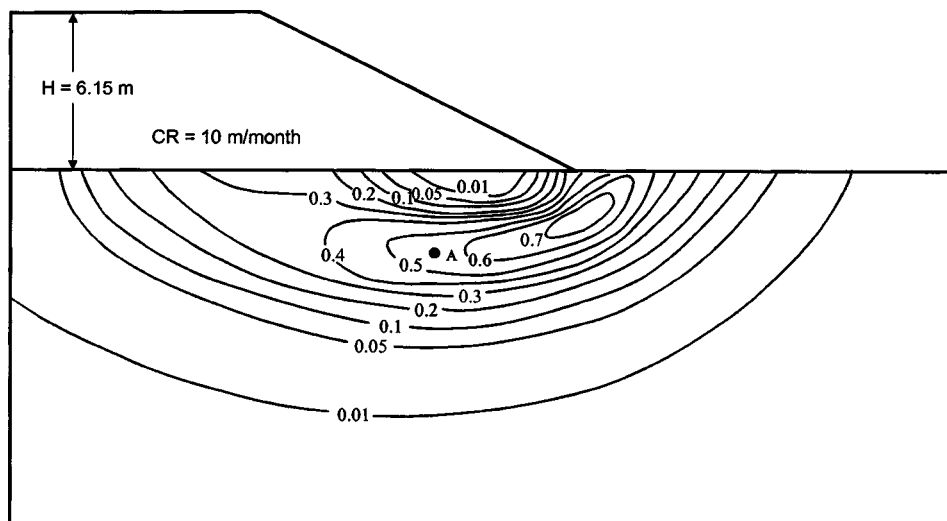


**Fig. 5.** Contours of strain rate (%/h) at onset of failure for embankment over Soil C-R1 ( $H_f=6.15$  m)

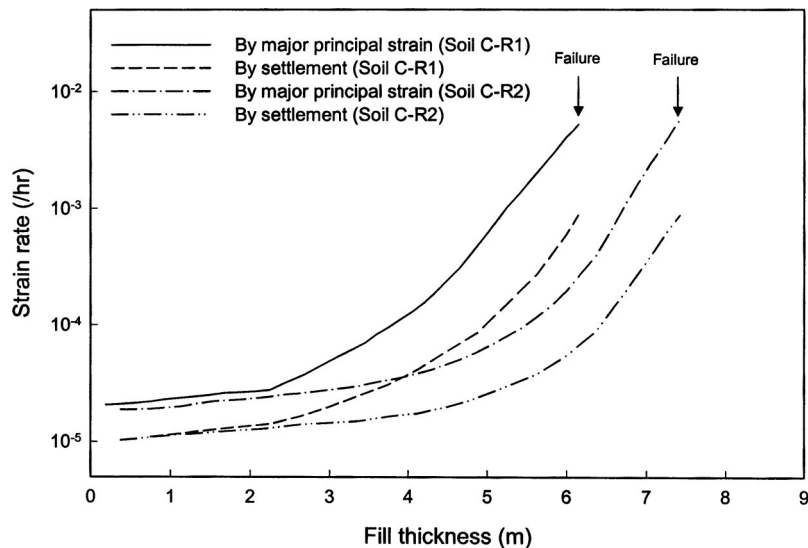


Fig. 6. Strain rate at Point A during construction of unreinforced embankment with CR=10 m/month

When an embankment experiences delayed progressive failure, the mobilized strength during this postconstruction failure will be different from the strength that had been mobilized at the end of construction due to the effect of creep and stress relaxation. The strain rate in the foundation will also change with time after the end of construction as shown in the following sections.

### Critical Stage and Critical Strain Rate

A number of investigators have reported that the excess pore pressure in soft clay foundations either remained essentially constant for a significant period or increased following embankment construction and that failure occurred during the postconstruction period rather than during or at the end of construction as typically expected for nonrate sensitive soils (Crooks et al. 1984; Keenan et al. 1986; Kabbaj et al. 1988; Rowe et al. 1996). Thus, both these previous field observations and theoretical analyses (Li 2000) have indicated that the immediate end of construction is not necessarily the most critical point in time with respect to the stability of embankments on rate sensitive foundation soils. This critical point in time (called the “critical stage” herein) corresponds to the time when the mobilized shear strength along the potential slip surface is at a minimum. To illustrate that this does not necessarily correspond to the end of construction, Fig. 7 shows the calculated effective stress paths at two locations A and B during and after the construction of a 5-m-high reinforced ( $J = 2,000$  kN/m) embankment over Soil C-R1.

During the initial elastic loading, the stress paths were nearly vertical (Fig. 7). After the soil became viscoplastic (the stress path passed the static yield envelope), the stress paths moved along a series of dynamic yield envelopes towards the failure envelope. Subsequently, the stress path at Point A moved slightly above the static failure envelope (the long-term strength envelope) due to rate effects. After the end of construction, pore pressure continued to increase and stress relaxation at constant volume [Fig. 7(b)] gave rise to a decrease in both deviatoric and mean effective stress until the stress path decreased to the point at which the lowest undrained shear strength was mobilized. This corresponds to the “critical stage” since the embankment is least stable at this stage. After the critical stage, there is an increase in effective

stresses due to consolidation, and the stress paths eventually moved away from the failure envelope as the pore pressures dissipate.

It is evident from Fig. 7 that two phenomena, namely, creep and stress relaxation, were occurring simultaneously in an essentially “undrained manner” [at constant volumetric strain,  $(\epsilon_1 + \epsilon_2 + \epsilon_3)/3$ ] for a period of time after the end of construction [Fig. 7(b)]. During creep and stress relaxation, the maximum shear strain  $(\epsilon_1 - \epsilon_3)/2$  increased significantly. The fact that stability deteriorates over a period of time after construction as implied by Fig. 7 is consistent with the field observations for embankments constructed on rate sensitive soils (Keenan et al. 1986; Kabbaj et al. 1988; Rowe et al. 1996).

The strain rate corresponding to the critical stage is defined herein as the critical strain rate. At the critical stage, the mobilized shear strength is the operational shear strength that governs the stability of the embankment. The critical strain rate can be used to estimate the operational undrained shear strength of foundation soil beneath embankment as will be shown in a later section.

### Critical Strain Rate and Influence Factors

A number of analyses were conducted to examine the potential effects of soil properties and construction rates on the critical strain rate. Fig. 8 shows the major principal strain rate at the typical Point A during and following construction up to the critical stage for reinforced embankments with reinforcement stiffness  $J = 1,000$  kN/m and  $J = 2,000$  kN/m, construction rates of 2, 10, and 30 m/month and two values of hydraulic conductivity ( $k_{v0} = 4 \times 10^{-10}$  m/s and  $2 \times 10^{-9}$  m/s) for the foundation Soil C-R1. In all cases, during construction, the strain rate was essentially constant with time when the soil was elastic with only a slight change due to geometric nonlinearity. Once the plastic zone began to develop, the logarithm of the strain rate increased approximately linearly with the logarithm of time. The strain rate reached the maximum at the end of construction and subsequently decreased with time during the postconstruction period.

Fig. 8(a) shows that although the construction rate significantly affected the strain rate at the end of construction (the 15-fold increase in construction rate from 2 m/month to 30 m/month

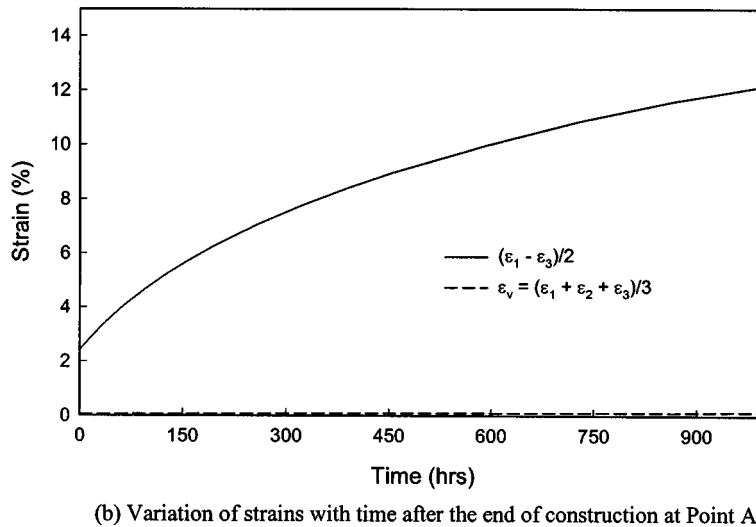
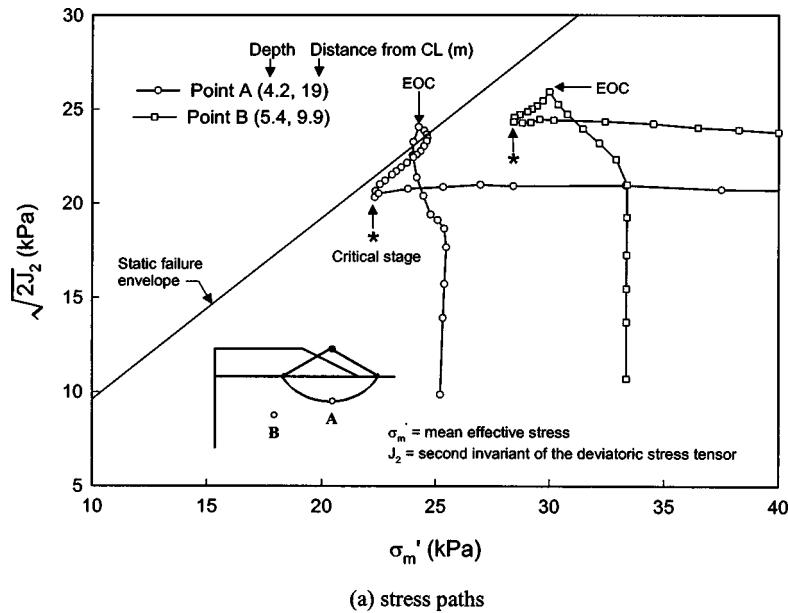


Fig. 7. Viscous behavior of Soil C-R1 under 5-m-thick reinforced embankment

resulted in an almost fourfold increase in strain rate from  $1.3 \times 10^{-4}/h$  to  $4.7 \times 10^{-4}/h$ , it did not significantly effect the strain rate at the critical stage. The critical strain rate was calculated to be around  $6 \times 10^{-5}/h$ , and was, to all practical purpose, the same for all three construction rates.

The effect of fill thickness on the strain rate is shown in Fig. 8(b) for the embankment  $H=5$  m with  $J=2,000$  kN/m and  $H=4.4$  m with 1,000 kN/m at the construction rate 10 m/month. For a given soil, the higher the embankment, the higher the intensity of shearing in the foundation soil and the higher the strain rate developed at the end of construction. However, the fill thickness did not significantly affect the strain rate at the critical stage. Fig. 8(b) also shows that a decrease in the hydraulic conductivity of the foundation soil from  $k_{vo}$  of  $2 \times 10^{-9}$  m/s to  $4 \times 10^{-10}$  m/s had no significant effect on the strain rate at the end of construction but did have some effect on the strain rate at critical stage. The foundation soil with the lower-hydraulic conductivity resulted in a slightly lower-critical strain rate (i.e.,  $4 \times 10^{-5}/h$ ).

Fig. 8 shows that although the strain rates at the end of construction might be very different due to factors such as embank-

ment height and construction rate, the strain rates decreased significantly with time after construction and the values were very similar at the critical stage with an average value of  $5 \times 10^{-5}/h$  for embankments constructed over Soil C-R1. The time to reach the critical stage was between about one and two months after the end of construction for the soil with  $k_{vo}=2 \times 10^{-9}$  m/s and  $k_{vo}=4 \times 10^{-10}$  m/s, respectively.

The factors examined in Fig. 8 for Soil C-R1 were also examined for Soil C-R2 and the critical strain rate of the foundation soil was found to be essentially independent on the construction rate and fill thickness. The critical strain rate was calculated to be  $1 \times 10^{-5}/h$  for this soil for the cases examined and the time to reach this critical strain rate was between about two and seven months. The longer time to reach the critical stage for Soil C-R2 than for Soil C-R1 is attributed to the lower value of viscoplastic fluidity parameter  $\gamma^{vp}$  of Soil C-R2 than that of Soil C-R1.

For the rate sensitive parameters examined here, the value of  $\gamma^{vp}$  for Soil C-R1 was 200 times higher than that for Soil C-R2 and the values of  $n$  for Soils C-R1 and C-R2 were 20 and 30, respectively. The rate sensitive parameters of Soils C-R1 and

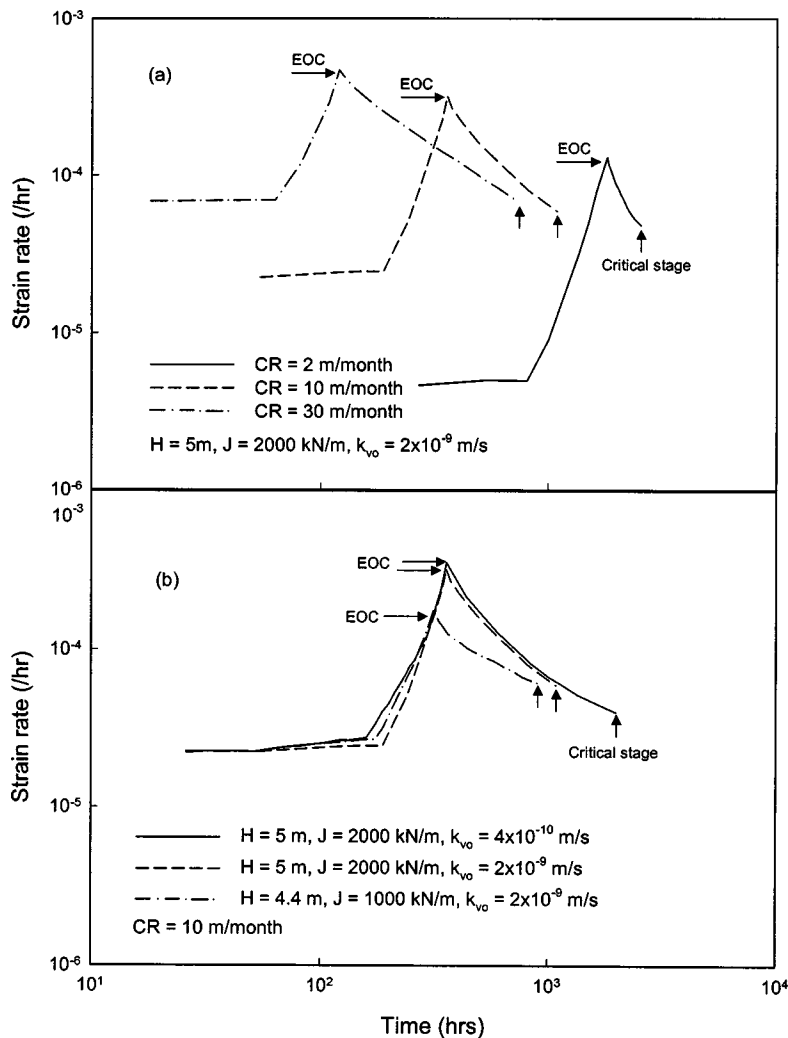


Fig. 8. Strain rate of Soil C-R1 at Point A during and after construction

C-R2 cover a wide range of practical conditions and yet the critical strain rate fell into a relative small range, between  $5 \times 10^{-5}/h$  and  $1 \times 10^{-5}/h$ . These findings suggest that for a typical range of rate sensitive soil deposits, the critical strain rate is likely to fall into a relative small range of values for typical construction rates.

### Operational Shear Strength of Rate Sensitive Soils

To illustrate that the operational shear strength of rate sensitive soil can be estimated using the critical strain rate, in this section, the construction of reinforced embankments over both Soils C-R1 and C-R2 was simulated using finite-element analyses, and then, the ratio of restoring to overturning moments (the equilibrium ratio) was calculated using limit-equilibrium analyses based on the undrained shear strength of soil calculated at the critical strain rate. The undrained shear strength was calculated based on finite-element simulations for plane strain compression tests at the critical strain rate of  $5 \times 10^{-3}/h$  and  $1 \times 10^{-5}/h$  for Soils C-R1 and C-R2, respectively.

Table 2 shows the comparison of results from finite-element (FE) analyses and limit-equilibrium (LE) analyses for embankments with reinforcement stiffness ranging from 500 kN/m to 4,000 kN/m. For each case, the reinforcement strain and force in reinforcement listed in the table are calculated at the critical stage

in the finite-element analyses. This force given by the FE analysis was used as the reinforcing force in the LE analysis to calculate the equilibrium ratio. For a perfect agreement between the LE and FE results, the equilibrium ratio would be equal to one when the shear strength of soil is mobilized along the potential failure plane. The equilibrium ratio calculated in the limit-equilibrium analyses was between 0.94 and 1.0 which agrees very well with the finite-element results and to the extent if the approach is in error, it is on the conservative side. This indicates that the undrained shear strength calculated based on the critical strain rate and used in the LE analyses reasonably represented the mobilized shear strength in the FE analyses at the critical stage (the operational shear strength) for the foundation soils examined.

### Reinforcement Strains

To examine the short-term and long-term reinforcement strains under different conditions, simulations of embankment construction to the heights given in Table 2 were performed using different construction rates and different hydraulic conductivities for the foundation soils. Fig. 9 shows the development of the maximum reinforcement strain from beginning of construction to 95% consolidation for 4.15 and 5.75-m-high embankments with reinforcement stiffness 500 and 4,000 kN/m, respectively, over foundation Soil C-R1. It was found that the maximum reinforcement

**Table 2.** Comparison of Results from Finite-Element Analyses and Limit-Equilibrium Analyses based on Critical Stage Concept ( $k_{vo}=4 \times 10^{-10}$  m/s; Construction Rate= 10 m/month)

	Finite-Element Analyses			Limit-Equilibrium Analyses		
	$H^a$ (m)	$J^b$ (kN/m)	$\varepsilon^c$ (%)	$T^d$ (kN/m)	$\varepsilon_c^e$ ( $h^{-1}$ )	ERAT <sup>f</sup> (—)
Soil C-R1	4.15	5,00	4.64	23	$5 \times 10^{-5}$	0.94
Soil C-R1	4.4	1,000	4.58	46	$5 \times 10^{-5}$	0.94
Soil C-R1	5	2,000	5.34	107	$5 \times 10^{-5}$	0.94
Soil C-R1	5.75	4,000	5.04	201	$5 \times 10^{-5}$	0.95
Soil C-R2	5.0	500	3.7	18	$1 \times 10^{-5}$	0.98
Soil C-R2	5.25	1,000	3.9	39	$1 \times 10^{-5}$	0.98
Soil C-R2	6.0	2,000	5.3	106	$1 \times 10^{-5}$	0.98
Soil C-R2	6.65	4,000	5.0	200	$1 \times 10^{-5}$	1.00
Soil A-R1	4.0	2,000	5.95	119	$2 \times 10^{-5}$	0.94
Soil A-R2	4.5	2,000	4.13	83	$5 \times 10^{-6}$	0.93
Soil B-R1	5.0	2,000	5.34	107	$4 \times 10^{-5}$	0.94
Soil B-R2	6.3	2,000	5.04	201	$1 \times 10^{-5}$	0.95

<sup>a</sup> $H$ =embankment fill thickness.

<sup>b</sup> $J$ =reinforcement stiffness.

<sup>c</sup> $\varepsilon$ = maximum reinforcement strain developed at critical stage.

<sup>d</sup> $T$ =reinforcing force.

<sup>e</sup> $\varepsilon_c$ =critical strain rate.

<sup>f</sup>ERAT=equilibrium ratio.

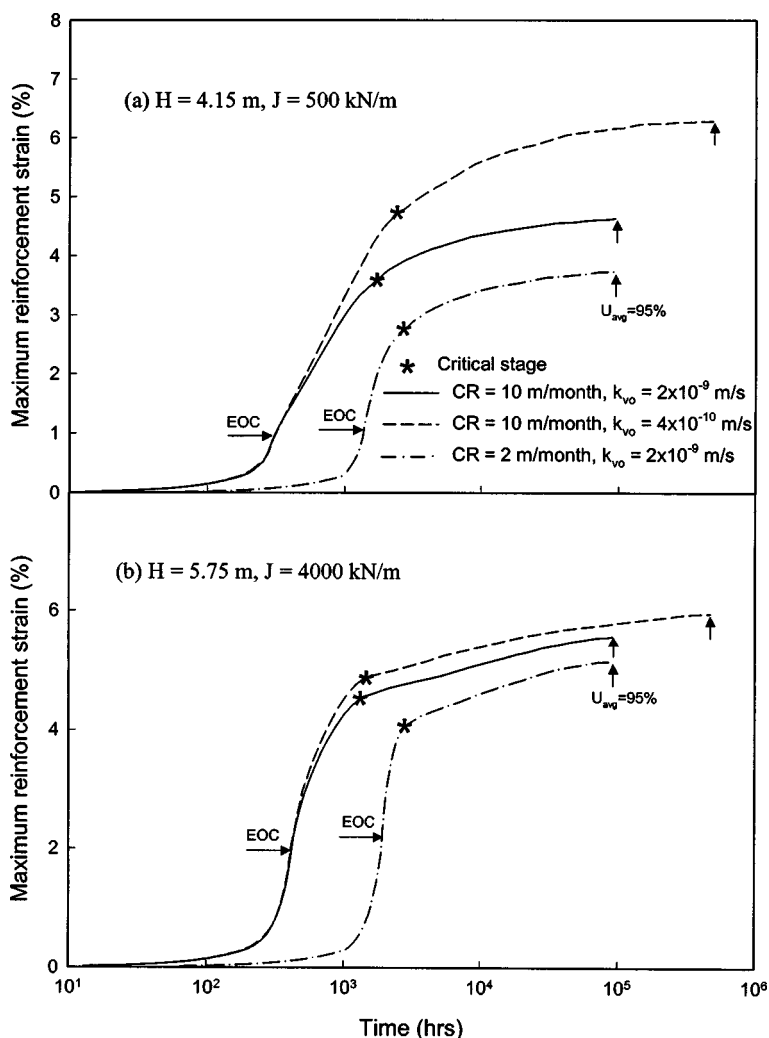


**Fig. 9.** Reinforcement strains developed during short term and long term for embankments over Soil C-R1

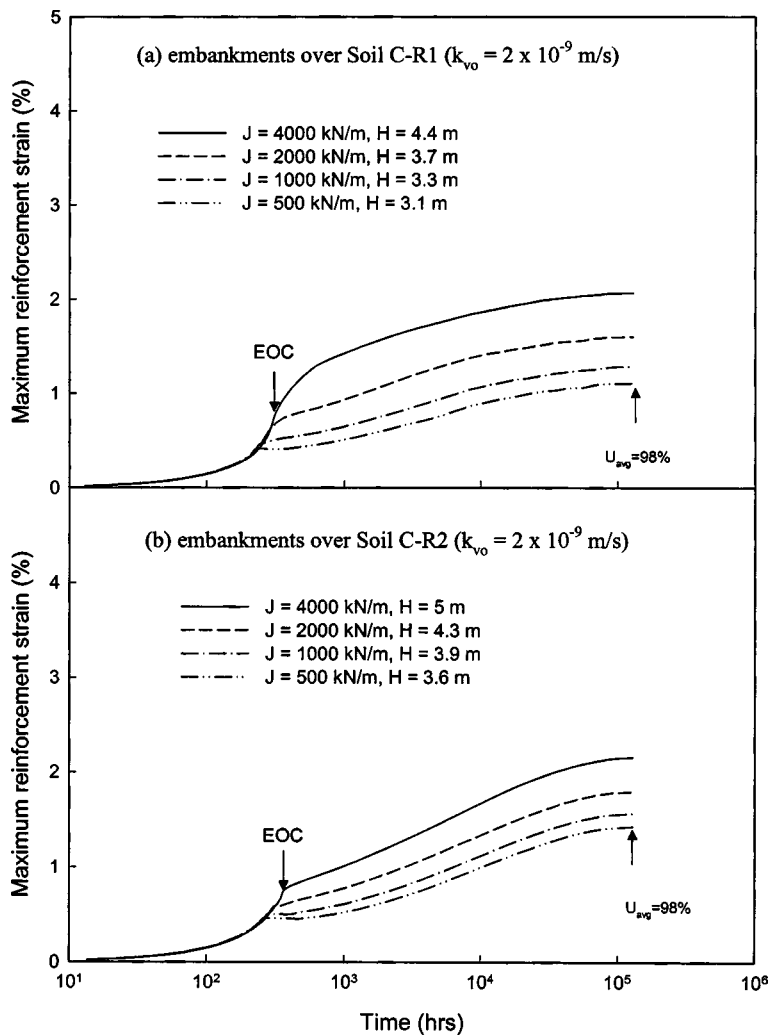


Fig. 10. Reinforcement strains developed during short term and long term for under working conditions

strains for these cases were relatively small at the end of construction and increased significantly after construction but prior to reaching the critical stage (denoted by an asterisk in Fig. 9). After the critical stage, the reinforcement strain increased slowly with time due to further creep and consolidation of the foundation soil. The long-term increase in reinforcement strain after the critical stage and before 95% consolidation stage was in the range from 0.9% for  $J=4,000$  kN/m to 1.7% for  $J=500$  kN/m. It is evident in Fig. 9 that the hydraulic conductivity of the foundation soil had an effect on the both short-term and long-term reinforcement strain with the higher-hydraulic conductivity giving rise to the slightly faster dissipation of excess pore pressure and smaller reinforcement strains. It is also evident that a slower construction rate resulted in a lower reinforcement strain both at the critical stage and in the long term.

#### Behavior of Reinforced Embankments under Working Conditions

The behavior of a reinforced embankment under working conditions is examined in this section using the critical stage and critical strain rate concept. Based on this concept, the embankment stability is most critical at the end of undrained creep and stress relaxation of the foundation soil (when the mean effective stress and strength are the lowest) and the shear strength measured at

the critical strain rate gives the operational strength of foundation soil. For the foundation soils examined, the undrained shear strength profile was first calculated using a critical strain rate of  $5 \times 10^{-5}/h$  and  $1 \times 10^{-5}/h$  for Soils C-R1 and C-R2, respectively. Based on the limit state design philosophy (Becker 1996; McGown et al. 1998), the limit-equilibrium program REAP (Mylleville and Rowe 1988) was used to calculate the allowable embankment height for an ERAT of 1.0 (the factored resistance moment being equal to factored overturning moment) assuming a reinforcement force corresponding to an allowable strain of 5%. For a partial factor  $f_{c1}=1.3$  for the foundation soil undrained shear strength,  $f_{c2}=1.0$  for the fill/foundation interface strength,  $f_{\phi}=1.2$  for both the embankment fill strength and reinforcement/fill interface strength parameters  $\tan \phi$ , and  $f_{\gamma}=1.0$  for the unit weight of the embankment fill, the calculated allowable embankment heights were 3.1, 3.3, 3.7, and 4.4 m for Soil C-R1 and 3.6, 3.9, 4.3, and 5.0 m for Soil C-R2 with reinforcement stiffness of 500, 1,000, 2,000, and 4,000 kN/m, respectively. The embankments were constructed to these heights at a rate of 10 m/month in finite-element analyses.

Fig. 10 shows the maximum reinforcement strains during and after construction up to 98% consolidation of the foundation soil. The increase in reinforcement strain after construction was between 1.3% for a 4.4-m-high embankment ( $J=4,000$  kN/m) and

0.6% for 3.1-m-high embankment ( $J = 500 \text{ kN/m}$ ) over Soil C-R1 ( $k_{vo} = 2 \times 10^{-9} \text{ m/s}$ ). For embankments over Soil C-R2 ( $k_{vo} = 2 \times 10^{-9} \text{ m/s}$ ), the long-term increase in reinforcement strain between the end of construction and 98% consolidation was between 1.4% for a 5.0-m-high embankment ( $J = 4,000 \text{ kN/m}$ ) and 1% for 3.6-m-high embankment ( $J = 500 \text{ kN/m}$ ). The mobilized maximum reinforcement strain under working conditions in the long term was less than 2.2% for the cases examined. Since shear intensity significantly influences the creep of soil, for a lower embankment on a given soil, the corresponding lower shear intensity would give a lower long-term creep induced reinforcement strain.

### Proposed Correction Factor for Use in Design of Reinforced Embankments

The importance of strain rate effects on embankment stability problems is discussed by Bjerrum (1973), Lo et al. (1976), Tavenas and Leroueil (1980), and Leroueil and Marques (1996). The strain rates used in field vane tests (Bjerrum 1972) and laboratory tests (Bishop and Henkel 1962; Germaine and Ladd 1988) may be much faster than the strain rates (as shown in the previous section) at which the foundation soil deforms under embankment loadings. The design of reinforced embankments based on the measured undrained shear strength of the foundation soil without correction may lead to a significant increase in reinforcement strain during postconstruction or failure of both the reinforcement and embankment (Li 2000). To adjust the measured undrained shear strength to a design value, the proposed correction factor is based on the calculated in situ strain rates and a power function that can reasonably correlate the undrained shear strength at different strain rates (Hinchberger 1996; Soga and Mitchell 1996), namely

$$\frac{s_{uf}}{s_u} = \mu = \left( \frac{\dot{\epsilon}_f}{\dot{\epsilon}} \right)^{1/m} \quad (1)$$

where  $s_{uf}$  = field operational undrained shear strength corresponding to the strain rate at failure or critical stage,  $\dot{\epsilon}_f$ ;  $s_u$  = measured undrained shear strength at a constant strain rate  $\dot{\epsilon}$ ; and  $m$  = strain rate parameter. The values of  $m = 14$  and  $20$  are calibrated to be equivalent to values of rate parameter  $n$  of  $20$  and  $30$  for Soil C-R1 and Soil C-R2, respectively. The parameter  $m$  can be obtained by conducting two tests at different strain rates; however, the critical strain rate (or the strain rate at failure),  $\dot{\epsilon}_f$ , has to be chosen from the numerical analyses described earlier and further elaborated below.

For embankments that fail during construction, the strain rate at failure is approximately  $1 \times 10^{-2}/\text{h}$  as shown in Fig. 6. Therefore, the correction factor  $\mu$ , for the measured shear strength  $s_u$ , is given by

$$\mu = \left( \frac{1 \times 10^{-2}/\text{h}}{\dot{\epsilon}} \right)^{1/m} \quad (2)$$

The correction factor can be used to back calculate the mobilized undrained shear strength based on the measured strength for typical rate sensitive soils (with an increase in undrained shear strength 10–15% per log cycle strain rate). For example, this equation was used to calculate the operational undrained shear strength of the Sackville rate sensitive soil. The Sackville test embankment was reinforced using a geotextile with an ultimate strength of  $212 \text{ kN/m}$  and the reinforcement failed shortly after the construction of the embankment to a fill thickness of  $8.2 \text{ m}$

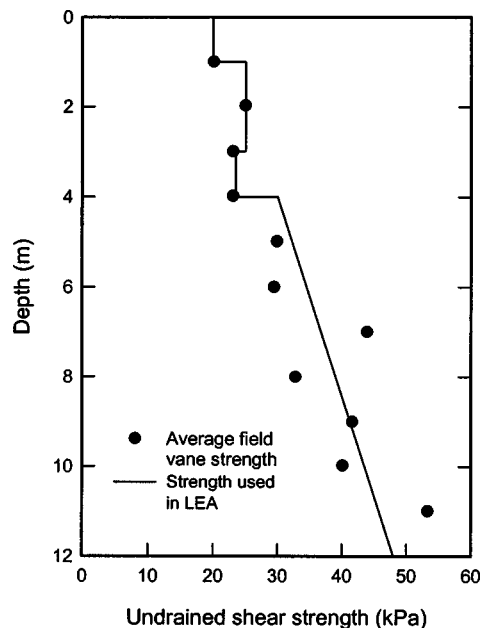


Fig. 11. Undrained shear strength of Sackville foundation soil

(Gnanendran 1993; Rowe et al. 1996). The undrained shear strength measured from field vane tests (with an assumed equivalent axial strain rate of  $1\% \text{ min}$ ) are shown in Fig. 11 and strain rate parameter  $m$  for the Sackville soil is  $14$ . Based on Eq. (2), the correction factor  $\mu$  was calculated to be  $0.75$ . Using the corrected field vane strength by applying  $\mu = 0.75$ , the calculated ratio of the restoring moment to the overturning moment was  $0.97$ , which implies that failure would occur. Thus, the limit-equilibrium analysis indicates the operational undrained shear strength of the Sackville rate sensitive soil at embankment failure shortly after construction could be reasonably estimated by applying Eq. (2) ( $\mu = 0.75$ ) to the field vane strength. For the Sackville soil with a plasticity index of  $19\%$ , the Bjerrum's correction factor is  $1.0$ , and hence even with the application of Bjerrum's correction there is an overestimate of the operational strength.

It has been shown in the previous section that the stability of embankments over rate sensitive soils may deteriorate with time over periods ranging between a few weeks and a few months even though the embankments are stable at the end of construction. For such cases, the correction factor for undrained shear strength should be based on the values of critical strain rates.

The critical strain rates of Soils C-R1 and C-R2 have been calculated and found to be insensitive to the construction rate. To further investigate the possible effect of different rate sensitive soils on the critical strain rate, a hypothetical Soil C with viscous parameters R3 ( $n = 30$  and  $\gamma^{vp} = 2 \times 10^{-5}/\text{h}$ ) and Soils A and B with viscous parameters R1 ( $n = 20$  and  $\gamma^{vp} = 2 \times 10^{-5}/\text{h}$ ) and R2 ( $n = 30$  and  $\gamma^{vp} = 1 \times 10^{-7}/\text{h}$ ) were also examined. The embankments over these soils were reinforced with reinforcement with  $J = 2,000 \text{ kN/m}$  and constructed to heights limited by an allowable reinforcement strain of  $5\%$ . From the construction of a  $4.7\text{-m}$ -high reinforced embankment over Soil C-R3 at a rate  $10 \text{ m/month}$ , the critical strain rate was found to be  $2 \times 10^{-5}/\text{h}$ , which is between the critical strain rates for Soils C-R1 and C-R2. For the embankments over viscous foundation Soils A and B, the critical strain rate were calculated and shown in Table 2.

As can be seen in Table 2, even though viscous Soils A, B, and C have different preconsolidation pressures, the values of critical

strain rates of soils having the same viscous parameters are very similar. This implies that provided that the rate sensitive properties are the same, different foundation soils will deform at approximately the same rate at the critical stage. Since the soils examined in this paper with viscous parameters encompasses the typical range of rate sensitive soils reported in literature (Berre and Bjerrum 1973; Graham et al. 1983; Leroueil et al. 1985; Lefebvre and LeBoeuf 1987; Kulhawy and Mayne 1990; Hinchberger 1996; Soga and Mitchell 1996), it is concluded that for typical rate sensitive foundation soils the critical strain rate is in the range between  $5 \times 10^{-6}/\text{h}$  and  $5 \times 10^{-5}/\text{h}$ . Based on this range, a critical strain rate of  $1 \times 10^{-5}/\text{h}$  is used in the following equation proposed for preliminary design considerations for the embankment stability that may deteriorate with time over a few weeks or a few months after construction before significant consolidation:

$$\mu = \left( \frac{1 \times 10^{-5}/\text{h}}{\dot{\epsilon}} \right)^{1/m} \quad (3)$$

To illustrate the use of Eq. (3) to estimate the undrained shear strength that will be mobilized at critical stage, the undrained shear strength profile of Soil C-R2 at a reference strain rate of  $1 \times 10^{-2}/\text{h}$  was corrected using the value of  $\mu$  deduced from Eq. (3) (0.71 for  $m=20$  and  $\dot{\epsilon} = 1 \times 10^{-2}/\text{h}$ ). It was found that the corrected undrained shear strength profile agreed closely with the operational undrained shear strength (calculated in the previous section).

Graham et al. (1983) report that the influence of strain rate on undrained shear strength appears to be independent of test type. This implies that Eqs. (2) and (3) may be applied to different laboratory tests and field test results to estimate operational shear strength in assessing embankment stability. For the typical rate sensitive soil examined (say  $m=20$ ), the correction factors, based on Eq. (3), for triaxial compression undrained tests at a strain rate of  $0.5 \sim 1\%/\text{h}$  as recommended by Germaine and Ladd (1988), would be 0.71–0.73 (the operational undrained shear strength would be about 27–29% less than measured). The deterioration in stability after construction due to rate effects can be estimated by comparing Eqs. (2) and (3). For example, for the typical rate sensitive soil ( $m=20$ ), dividing Eq. (3) by Eq. (2) gives 0.71 which implies a 29% decrease in strength at the critical stage.

## Conclusions

The behavior of reinforced embankments constructed over rate sensitive foundation soils was investigated using numerical analyses. The strain rate at which the foundation soil would deform during and after construction was investigated. The important factors examined include viscoplastic properties, foundation soil profiles, construction rates, and reinforcement stiffness. The following summarizes the salient findings:

1. When embankments are constructed over rate sensitive soils, the stability decreases for a period of time after construction due to the creep and stress relaxation of the foundation soil. The critical stage can be identified to be at the end of essentially undrained creep and stress relaxation of foundation soils before significant consolidation occurs. The more viscous the soil the longer it takes time to reach the critical stage.
2. The operational strength of foundation soils can be estimated using the critical strain rate, namely, the strain rate corresponding to the critical stage.

3. The viscous properties of soils are the dominant factors that affect the critical strain rate. Construction rates and the stress history of the foundation soil have an insignificant effect on the critical strain rate for the cases examined. Based on the embankments examined, it is concluded that the critical strain rate is between  $5 \times 10^{-6}/\text{h}$  and  $5 \times 10^{-5}/\text{h}$  for a range of rate sensitive soils with a typical value of  $1 \times 10^{-5}/\text{h}$  for a typical rate sensitive soil.
4. The proposed correction factor allowing for strain rate effects on the shear strength of rate sensitive soils worked reasonably well for the case examined and warrants further investigation using additional field cases.

## Acknowledgment

The research reported in this paper was funded by the Natural Sciences and Engineering Research Council of Canada.

## References

- Adachi, T., and Oka, F. (1982). "Constitutive equations for normally consolidated clay based on elasto-viscoplasticity." *Soils Found.*, 22(4), 57–70.
- Becker, D. E. (1996). "Eighteenth Canadian geotechnical colloquium: Limit states design for foundations. Part I. An overview of the foundation design process." *Can. Geotech. J.*, 33(6), 956–983.
- Berre, T. and Bjerrum, L. (1973). "Shear strength of normally consolidated clays." *Proc., 8th Int. Conf. on Soil Mechanics and Foundation Engineering*, Moscow, 1, 39–49.
- Biot, M. A. (1941). "General theory of three-dimensional consolidation." *J. Appl. Phys.*, 12, 155–164.
- Bishop, A. W., and Henkel, D. J. (1962). *The measurement of soil properties in the triaxial test*, 2nd Ed., Edward Arnold LTD, London.
- Bjerrum, L. (1972). "Embankments on soft ground." *Proc., ASCE Specialty Conf. on Earth and Earth-Supported Structures*, Purdue Univ., West Lafayette, Ind., 2, 1–54.
- Bjerrum, L. (1973). "Problems of soil mechanics and construction on soft clays." *Proc., 8th Int. Conf. on Soil Mechanics and Foundation Engineering*, Moscow, 3, 111–159.
- Carter, J. P., and Balaam, N. P. (1990). *AFENA—A general finite element algorithm: Users manual*, School of Civil and Mining Engineering, Univ. of Sydney, Australia.
- Casagrande, A., and Wilson, S. D. (1951). "Effect of rate of loading on the strength of clays and shales at constant water content." *Geotechnique*, 2, 251–263.
- Chen, W. F., and Mizuno, E. (1990). "Nonlinear analysis in soil mechanics—Theory and implementation." Elsevier, New York.
- Crooks, J. H. A., Becker, D. E., Jeffries, M. G., and McKenzie, K. (1984). "Yield behaviour and consolidation. I: Pore pressure response." *Proc., ASCE Symposium on Sedimentation Consolidation Models, Prediction and Validation*, San Francisco, 356–381.
- Dascal, O., and Tournier, J. P. (1975). "Embankment on soft and sensitive clay foundation." *J. Geotech. Eng. Div., Am. Soc. Civ. Eng.*, 101(3), 297–3144.
- Davis, E. H. (1968). "Soil mechanics—Selected topics, In: Theories of plasticity and failure of soil masses." I. K. Lee, ed., Butterworths, London, Chap. 6.
- Desai, C. S., and Zhang, D. (1987). "Viscoplastic model for geologic materials with generalized flow rule." *Int. J. Numer. Analyt. Meth. Geomech.*, 11, 603–620.
- Fisher, D. G., Rowe, R. K., and Lo, K. Y. (1982). "Prediction of the second stage behaviour of Gloucester test fill Part 1—Predictions; Part 2—Method of analysis." *GEOT-3-82, GEOT-4-82*, Faculty of Engineering Science, Univ. of Western Ontario, Canada.

- Germaine, J. T., and Ladd, C. C. (1988). "Triaxial testing of saturated cohesive soils. Advanced triaxial testing of soil and rock." *ASTM Special Tech. Publication No. 977*, ASTM, Philadelphia, 421–459.
- Gnanendran, C. T. (1993). "Behaviour of geotextile reinforced embankments on soft soils" PhD thesis, Faculty of Graduate Studies, Univ. of Western Ontario, Canada.
- Graham, J., Crooks, J. H. A., and Bell, A. L. (1983). "Time effects on the stress-strain behaviour of natural soft clays." *Geotechnique*, 33, 727–340.
- Hinchberger, S. D. (1996). "The behaviour of reinforced and unreinforced embankments on rate sensitive clayey foundations." PhD thesis, Faculty of Graduate Studies, Univ. of Western Ontario, Canada.
- Hinchberger, S. D., and Rowe, R. K. (1998). "Modelling the rate sensitive characteristics of the Gloucester foundation soil." *Can. Geotech. J.*, 35(5), 769–789.
- Holtz, R. D., Christopher, B. R., and Berg, R. R. (1997). *Geosynthetic engineering*, BiTech, Richmond, British Columbia, Canada.
- Huang, T. K., and Chen, W. F. (1990). "Simple procedure for determining cap-plasticity-model parameters." *J. Geotech. Eng.*, 116(3), 492–513.
- Humphrey, D. N., and Holtz, R. D. (1988). "Cap parameters for clayey soils." *Numerical methods in geomechanics*, G. Swoboda, ed., *Proc., 6th Int. Conf. on Numerical Methods in Geomechanics*, Balkema, Rotterdam, The Netherlands, 441–446.
- Janbu, N. (1963). "Soil compressibility as determined by oedometer and triaxial tests." *Proc., European Conf. on Soil Mechanics and Foundation Engineering*, Wiesbaden, Germany, 1, 19–25.
- Jewell, R. A. (1982). "A limit equilibrium design method for reinforced embankments on soft foundations." *Proc., 2nd Int. Conf. on Geotextiles*, Las Vegas, 4, 671–676.
- Kabbaj, M., Tavenas, F., and Leroueil, S. (1988). "In situ and laboratory stress-strain relationships." *Geotechnique*, 38(1), 83–100.
- Katona, M. G., and Mulert, M. A. (1984). "A viscoplastic cap model for soils and rock." *Mechanics of engineering materials*, C. S. Desai and R. H. Gallagher, eds., Wiley, 335–350.
- Keenan, G. H., Landva, A. O., Valsangkar, A. J., and Comier, R. S. (1986). "Performance and failure of test embankment on organic silty clay." *Proc., Conf. on Building on Marginal and Derelict Land, Glasgow Institute of Civil Engineering*, 2, 417–428.
- Koerner, R. M. (1997). *Designing with geosynthetics*, 4th Ed., Prentice-Hall, Englewood Cliffs, N.J.
- Kulhawy, F. H., and Mayne, P. W. (1990). *Manual on estimation soil properties for foundation design*, Electric Power Research Institute, Palo Alto, Calif.
- Ladd, C. C. (1991). "Stability evaluation during staged construction." *J. Geotech. Eng.*, 117(4), 540–615.
- Ladd, C. C., and Foott, R. (1974). "New Design procedure for stability of soft clays." *J. Geotech. Eng. Div., Am. Soc. Civ. Eng.*, 100(7), 763–786.
- Larsson, R. (1980). "Undrained shear strength in stability calculations of embankments and foundations on soft clays." *Can. Geotech. J.*, 17(4), 591–602.
- Lefebvre, G., and LeBoeuf, D. (1987). "Rate effects and cyclic loading of sensitive clays." *J. Geotech. Eng.*, 113(5), 476–489.
- Leroueil, S., Kabbaj, M., Tavenas, F., and Bouchard, R. (1985). "Stress-strain-strain rate relation of the compressibility of sensitive natural clays." *Geotechnique*, 35(2), 159–180.
- Leroueil, S., and Marques, M. E. S. (1996). "Importance of strain rate and temperature effects in geotechnical engineering." *Proc., 1996 ASCE National Convention*, Washington, D.C., Geotechnique Spec. Publ. No. 61, 1–60.
- Leshchinsky, D. (1987). "Short-term stability of reinforced embankment over clayey foundations." *Soils Found.*, 27(3), 43–57.
- Li, A. L. (2000). "Time dependent behaviour of reinforced embankments on soft foundations" PhD thesis, Faculty of Graduate Studies, Univ. of Western Ontario, Canada.
- Lo, K. Y., Bozozuk, M., and Law, K. T. (1976). "Settlement analysis of Gloucester test fill." *Can. Geotech. J.*, 13(4), 339–354.
- Lo, K. Y., and Morin, J. P. (1972). "Strength anisotropy and time effects of two sensitive clays." *Can. Geotech. J.*, 9(3), 261–277.
- McCarron, W. O., and Chen, W. F. (1987). "A capped plasticity model applied to Boston blue clay." *Can. Geotech. J.*, 24(4), 630–644.
- McGown, A., Andrawes, K. Z., Pradhan, S., and Khan, A. J. (1998). "Limit state design of geosynthetic reinforced soil structures." *6th Int. Conf. on Geosynthetics*, 144–179.
- Mylleville, B. L. J., and Rowe, R. K. (1988). "Simplified undrained stability analysis for use in the design of steel reinforced embankments on soft foundations." *GEOT-3-88*, 73, Faculty of Engineering Science, Univ. of Western Ontario, Canada.
- Perloff, W. H., and Osterberg, J. O. (1963). "The effect of strain rate on the undrained shear strength of cohesive soils." *Proc., 2nd Pan-American Conf. on Soil Mechanics and Foundation Engineering*, Rio de Janeiro, Brazil, 1, 103–128.
- Perzyna, P. (1963). "The constitutive equations for work-hardening and rate sensitive plastic materials." *Proc., Vibrational Problems*, Warsaw, Poland 4(3), 281–290.
- Rowe, R. K., Gnanendran, C. T., Landva, A. O., and Valsangkar, A. J. (1996). "Calculated and observed behaviour of a reinforced embankment over soft compressible soil." *Can. Geotech. J.*, 33(2), 324–338.
- Rowe, R. K., and Hinchberger, S. D. (1998). "The significance of rate effects in modelling the Sackville test embankment." *Can. Geotech. J.*, 35(3), 500–516.
- Rowe, R. K., and Li, A. L. (2000). "Behaviour of reinforced embankments on soft rate sensitive soils." *GEOT-10-00*, 52 p, Faculty of Engineering Science, Univ. of Western Ontario, Canada.
- Rowe, R. K., and Mylleville, B. L. J. (1996). "A geogrid reinforced embankment on peat over organic silt: A case history." *Can. Geotech. J.*, 33(1), 106–122.
- Rowe, R. K., and Soderman, K. L. (1984). "Comparison of predicted and observed behaviour of two test embankments." *Geotext. Geomembr.*, 1(2), 143–160.
- Rowe, R. K., and Soderman, K. L. (1987). "Stabilization of very soft soils using high strength geosynthetics: The role of finite element analyses." *Geotext. Geomembr.*, 6(1–3), 53–80.
- Schiffman, R. L., Chen, A. T-F., and Jordan, J. C. (1969). "An analysis of consolidation theories." *J. Soil Mech. Found. Div.*, 95(SM1), 285–312.
- Schmertmann, J. H. (1975). "Measurement of in situ shear strength. State of the art report." *Proc., ASCE Conf. on In-situ Measurement of Soil Parameters*, 2, 56–137.
- Sheahan, T. C., Ladd, C. C., and Germaine, J. T. (1996). "Rate-dependent undrained shear behaviour of saturated clay." *J. Geotech. Eng.*, 122(2), 99–108.
- Soga, K., and Mitchell, J. K. (1996). "Rate-dependent deformation of structured natural clays." *Proc., 1996 ASCE National Convention*, Washington, D.C., Geotechnique Spec. Publ. No. 61, 243–257.
- Taylor, D. W. (1948). *Fundamentals of soil mechanics*, Wiley, New York.
- Tavenas, F., and Leroueil, S. (1980). "The behaviour of embankments on clay foundations." *Can. Geotech. J.*, 17(2), 236–260.
- Terzaghi, K. (1931). "The static rigidity of plastic clays." *J. Rheol.*, 2(3), 253–262.
- Trak, B., La Rochelle, P., Tavenas, F., Leroueil, S., and Roy, M. (1980). "A new approach to the stability analysis of embankments on sensitive clays." *Can. Geotech. J.*, 17(4), 526–544.